



# Conserved use of the sodium/bile acid cotransporter (NTCP) as an entry receptor by hepatitis B virus and domestic cat hepadnavirus

Maya Shofa<sup>a,b</sup>, Akiho Ohkawa<sup>a</sup>, Yasuyuki Kaneko<sup>a,c</sup>, Akatsuki Saito<sup>a,b,d,\*</sup>

<sup>a</sup> Department of Veterinary Science, University of Miyazaki, Miyazaki, Miyazaki, 8892192, Japan

<sup>b</sup> Graduate School of Medicine and Veterinary Medicine, University of Miyazaki, Miyazaki, Miyazaki, 8891692, Japan

<sup>c</sup> Veterinary Teaching Hospital, University of Miyazaki, Miyazaki, Miyazaki, 8892192, Japan

<sup>d</sup> Center for Animal Disease Control, University of Miyazaki, Miyazaki, Miyazaki, 8892192, Japan

## ARTICLE INFO

### Keywords:

Hepadnavirus  
Hepatitis B virus (HBV)  
Domestic cat hepadnavirus  
Sodium/bile acid cotransporter (NTCP)

## ABSTRACT

The *Orthohepadnavirus* genus includes hepatitis B virus (HBV) that can cause chronic hepatitis and hepatocarcinoma in humans. Recently, a novel hepadnavirus in cats, domestic cat hepadnavirus (DCH), was identified that is genetically close to HBV. DCH infection is associated with chronic hepatitis in cats, suggesting a similarity with HBV pathogenesis and the potential to use DCH as a novel animal model for HBV research. HBV is shown to use the sodium/bile acid cotransporter (NTCP) as a major cell entry receptor, but the equivalent receptor for DCH remains unknown. Here we sought to identify the entry receptor for DCH. HBV- and DCH-derived preS1 peptides efficiently bound to both human and cat NTCPs, and residue 158 of NTCP proteins determined the species-specific binding of the DCH preS1 peptide. Myrludex B, an HBV entry inhibitor, blocked the binding of the DCH preS1 peptide. Thus, DCH and HBV may share cell entry molecules, suggesting a possibility of inter-species transmission. Furthermore, our study suggests that DCH can be useful as a novel model for HBV research.

## 1. Introduction

*Hepadnaviridae* are enveloped DNA viruses that have a partially double-stranded, circular DNA genome and a broad host tropism, including mammals, reptiles, frogs, birds, and fish (Magnius et al., 2020). Human infection with hepatitis B virus (HBV), a member of the *Orthohepadnavirus* genus, can induce chronic liver damage, including cirrhosis and hepatocellular carcinoma, and, despite effective vaccines being available, eradicating chronic infections can be challenging. Therefore, suitable HBV animal models are required to advance therapeutic outcomes. Chimpanzees are now unavailable as an animal model for HBV infection, and infection models using HBV-like viruses in woodchuck, ground squirrel, and duck have consequently been investigated (Delmas et al., 2002; Guo et al., 2000; Jilbert et al., 1992; Kajino et al., 1994; Marion et al., 2002). Although treeshrews (*Tupaia*) are used as an animal model, the limited availability of research reagents may make it difficult to use this animal. Therefore, the development of a novel and convenient animal model is still required.

In 2018, an HBV-like virus, domestic cat hepadnavirus (DCH), was identified in domestic cats in Australia and was associated with feline chronic hepatitis (Aghazadeh et al., 2018), suggesting a similarity with

HBV pathogenesis. Subsequently, DCH was identified in other countries, including Italy (Lanave et al., 2019), Thailand (Piewbang et al., 2020), Malaysia (Anpuanandam et al., 2021), United Kingdom (Jeanes et al., 2022), United States (Stone et al., 2022), Hong Kong (Capozza et al., 2023), and Japan (Takahashi et al., 2022). DCH has a partially double-stranded, circular DNA genome of ~3,200 bases in length (Aghazadeh et al., 2018). As observed with other *Orthohepadnavirus* species, the genome of DCH encodes polymerase, surface, core, and X proteins. However, the viral replication mechanism of DCH is largely unknown, especially the entry into target cells.

HBV uses three envelope glycoproteins: Large (preS1 + preS2 + S), Middle (preS2 + S), and Small (S only) proteins for infection. Notably, the myristoylated preS1 domain is responsible for interaction with the cellular receptor (Engelke et al., 2006; Gripon et al., 2005; Le Seyec et al., 1999; Schulze et al., 2010). NTCP, a sodium-dependent bile acid symporter, is the major cell receptor for HBV (Yan et al., 2012). Therefore, considerable effort has been made to interrupt the interaction between preS1 and NTCP to develop an entry inhibitor. Myrludex B, a synthetic lipopeptide derived from the preS1 domain of the HBV envelope protein, specifically targets hepatocytes to efficiently block *de novo* HBV infection (Gripon et al., 2005; Schulze et al., 2010), and has

\* Corresponding author. Department of Veterinary Science, University of Miyazaki, Miyazaki, Miyazaki, 8892192, Japan.

E-mail address: [sakatsuki@cc.miyazaki-u.ac.jp](mailto:sakatsuki@cc.miyazaki-u.ac.jp) (A. Saito).

<https://doi.org/10.1016/j.antiviral.2023.105695>

Received 8 February 2023; Received in revised form 25 June 2023; Accepted 31 July 2023

Available online 1 August 2023

0166-3542/© 2023 The Authors. Published by Elsevier B.V. This is an open access article under the CC BY license (<http://creativecommons.org/licenses/by/4.0/>).

consequently received approval in Europe to treat patients.

In this study, we sought to use DCH as a model for HBV infection and investigated the entry pathway of DCH using the DCH-derived preS1 peptide. We demonstrated that the DCH-derived preS1 peptide efficiently binds to cat NTCP, and importantly, human NTCP. Furthermore, using Hepatitis D virus (HDV) particles enveloped with HBV and DCH-derived L proteins, we demonstrated that DCH utilizes human and cat NTCPs as a functional receptor. Consistent with findings with HBV (Takeuchi et al., 2019), the G158 residue of NTCP determines the species specificity of DCH, suggesting that the binding mode of preS1 and NTCP is conserved between HBV and DCH and that there is a potential risk of inter-species transmission of DCH. Myrcludex B potentially inhibited the binding of the DCH-derived preS1 peptide to human and cat NTCPs, suggesting that the mode of inhibition can be evaluated in DCH-infected cats. Overall, this study provides a promising strategy for establishing a novel animal model for HBV infection, which could help develop therapeutic measures in HBV-infected individuals.

## 2. Materials and methods

### 2.1. Plasmids

NTCP cDNA sequences of 18 animal species (Table 1) were synthesized (Twist Bioscience) with codon optimization for expression in human cells. Synthesized DNA sequences are summarized in Supplementary Table 1. For transient expression of NTCP, inserts encoding NTCP cDNA were cloned into a pCAGGS vector (Niwa et al., 1991) predigested with EcoRI-HF (NEB, Cat# R3101M) and NheI-HF (NEB, Cat# R3131M) using In-Fusion Snap Assembly Master Mix (TaKaRa, Cat# Z8947N). In addition, for stable expression of NTCP, inserts encoding NTCP cDNA of human, cat, and cynomolgus monkey were cloned into a pLVISIN-CMV Hyg vector (TaKaRa, Cat# 6182) predigested with NotI-HF (NEB, Cat# R3189L) and BamHI-HF (NEB, Cat# R3136L) using In-Fusion Snap Assembly Master Mix. Plasmids were amplified using NEB 5-alpha F'Iq Competent *Escherichia coli* (High Efficiency) (NEB, Cat# C2992H), and isolated with PureYield Plasmid Miniprep System (Promega, Cat# A1222). Sequences of all plasmids were verified using a SupreDye v3.1 Cycle Sequencing Kit (M&S TechnoSystems, Cat# 063001) with a Spectrum Compact CE System (Promega). psPAX2-IN/HiBIT was a kind gift from Dr. Kenzo Tokunaga (Ozono et al., 2020). pSVL (D3) was provided from Dr. John Taylor (Addgene, Cat# 29335; <http://n2t.net/addgene:29335>; RRID: Addgene\_29335) (Kuo et al., 1989). pMD2.G was a gift from Dr. Didier Trono (Addgene, Cat# 12259; <http://n2t.net/addgene:12259>; RRID: Addgene\_12259). pBS HBV-L (Zhang et al., 2022), a pBluescript plasmid (Alting-Mees and Short, 1989) expressing L protein of HBV (ayw subtype), was a kind gift

**Table 1**  
NTCP amino acid sequence of 18 animal species tested in this study.

Species	Common name	GenBank Acc. No
<i>Homo sapiens</i>	Human	NP 003040.1
<i>Felis catus</i>	Cat	XP 003987831.1
<i>Macaca fascicularis</i>	Cynomolgus monkey	XP 045252552.1
<i>Mus musculus</i>	Mouse	NP 001171032.1
<i>Aotus nancymaae</i>	Nancy Ma's night monkey	XP 012293622.1
<i>Leopardus geoffroyi</i>	Geoffroy's cat	XP 045304082.1
<i>Sus scrofa</i>	Pig	XP 001927730.1
<i>Panthera tigris</i>	Tiger	XP 007095203.2
<i>Saimiri sciureus</i>	Squirrel monkey	ALX72398.1
<i>Canis lupus familiaris</i>	Dog	XP 537494.2
<i>Tupaia belangeri</i>	Treeshrew	AFK93890.1
<i>Rhinolophus ferrumequinum</i>	Horseshoe bat	KAF6352409.1
<i>Pteropus alecto</i>	Black fruit bat	XP 006915243.1
<i>Bos taurus</i>	Cow	NP 001039804.1
<i>Marmota monax</i>	Woodchuck	XP 046316751.1
<i>Ictidomys tridecemlineatus</i>	Ground squirrel	XP 005322900.1
<i>Rattus norvegicus</i>	Rat	NP 058743.1
<i>Ornithorhynchus anatinus</i>	Platypus	XP 028932136.1

from Dr. Toru Okamoto.

### 2.2. Generation of plasmids encoding NTCPs mutants

To generate NTCP mutants, mutagenesis was performed via overlapping PCR using PrimeSTAR GXL DNA polymerase (TaKaRa, Cat# R050A) with the primers listed in Supplementary Table 2. The PCR protocol consisted of 35 cycles at 98 °C for 10 s, 60 °C for 15 s, and 68 °C for 1 min, followed by 68 °C for 7 min. Amplified PCR fragments encoding the intended mutation were cloned into a pCAGGS vector as described above. Plasmids were verified by sequencing.

### 2.3. Generation of plasmids encoding DCH L proteins

To generate plasmids encoding DCH L proteins, DCH (Rare) and DCH (Sydney)-derived sequences were synthesized by Twist Bioscience. Synthesized DNA sequences are summarized in Supplementary Table 3. These L protein sequences were cloned into a pBS HBV-L plasmid using In-Fusion Snap Assembly Master Mix to generate pBS DCH (Rare)-L plasmid and pBS DCH (Sydney)-L plasmid. Plasmids were verified by sequencing.

### 2.4. Cell culture

Lenti-X 293T cells (TaKaRa, Cat# Z2180N) and Huh7 cells (JCRB, Cat# JCRB0403) were cultured in Dulbecco's modified Eagle medium (DMEM) (Nacalai Tesque, Cat# 08458-16) supplemented with 10% fetal bovine serum and 1 × penicillin–streptomycin (Nacalai Tesque, Cat# 09367-34). We obtained primary human hepatocytes (PHHs) (Lonza, Cat# HUCPG) and the frozen cells were thawed using a Thawing medium (Lonza, Cat# MCHT50) according to the manufacturer's instruction. PHHs were plated in a Celltight C-1 Plate 96F plate (Wako, Cat# 631-26891) using HCMTM Hepatocyte Culture Medium BulletKit (Lonza, Cat# CC-3198) and Hepatocyte Plating Medium w/Supplement (Lonza, Cat# MP100) according to the manufacturer's protocol.

### 2.5. Generation of Huh7 cells stably expressing NTCP molecules

To prepare an HIV-1-based lentiviral vector, Lenti-X 293T cells (5 × 10<sup>5</sup>) were cotransfected with 0.8 μg psPAX2-IN/HiBIT, 0.8 μg pLVISIN-CMV Hyg-NTCP, and 0.4 μg pMD2.G plasmids using TransIT-293 Transfection Reagent (TaKaRa, Cat# V2700) in Opti-MEM I Reduced Serum Medium (Thermo Fisher Scientific, Cat# 31985062). The supernatant was filtered 2 days after transfection, and collected lentiviral vectors were used to infect Huh7 cells. Infected cells were cultured with 800 μg/mL Hygromycin B (Nacalai Tesque, Cat# 09287-84) for 6 days. Then, single-cell cloning was performed, and the expression level of NTCP in each clone was evaluated by western blotting.

### 2.6. preS1 peptide binding assay

Lipopeptide myr-47WT, a N-terminally myristoylated peptide comprising residues 2 to 47 of the preS1 region of HBV, and myr-47N9K, where Asn at position 9 is substituted with Lys, were synthesized by Scrum Co. (Tokyo, Japan). In addition, lipopeptide myr-47-DCH-WT, an N-terminal myristoylated peptide comprising residues 2 to 47 of the preS1 region of DCH, and myr-47-DCH-N9K were synthesized.

Huh7 cells (1 × 10<sup>6</sup>) were plated in a Celltight C-1 Plate 96F plate. After overnight incubation, cells (1 × 10<sup>4</sup>) were cotransfected with 50 ng pCAGGS-NTCP plasmids together with 50 ng pCAGGS-mCherry2 plasmid using TransIT-X2 Dynamic Delivery System (TaKaRa, Cat# V6100) in Opti-MEM I Reduced Serum Medium to normalize the transfection efficiency. At 24 h after transfection, cells were inoculated with the 400 nM corresponding peptides and incubated at 37 °C for 60 min. After two washes with Gibco William's E Medium (Thermo Fisher Scientific, Cat# A1217601), cells were observed under the EVOS M7000

Imaging System (Thermo Fisher Scientific). The cells were also analyzed via the Attune NxT Flow Cytometer (Thermo Fisher Scientific). The mCherry2-positive population was gated, and the percentage of FAM-positive (preS1 peptide binding positive) cells was analyzed using FlowJo v10.8.1 (Becton, Dickinson and Company) (Supplementary Fig. 1).

For the preS1 peptide binding assay on Huh7 cells stably expressing NTCP, Huh7 cells stably expressing NTCP ( $1 \times 10^6$ ) were plated in a Celltight C-1 Plate 96F plate. After overnight incubation, cells were used for preS1 peptide binding assay, as described above.

## 2.7. Quantification of mRNA level in PHHs transfected with DsiRNA targeting Ntcp

PHHs cultured ( $5 \times 10^5$ ) in a Celltight C-1 Plate 96F plate were transfected with 1 nM DsiRNA targeting *Ntcp* or negative control DsiRNA in TriFECTa RNAi Kit (IDT, hs.Ri.SLC10A1.13.1, 13.2, 13.3 REF#:107989675) using TransIT-X2 Dynamic Delivery System in Opti-MEM I Reduced Serum Medium. After overnight culture, mRNA expression was quantified by qRT-PCR using the CellAmp Direct RNA Prep Kit for RT-PCR (Real Time) (TaKaRa, Cat# 3732), One Step TB Green PrimeScript PLUS RT-PCR Kit (Perfect Real Time) (TaKaRa, Cat# RR096A), and primer pairs for human *Ntcp* (5'-GAAGACAAGGTGCCCTATAAA-3' and 5'-GGATTGAGGAGCATCCTATG-3') and human *Gapdh* (5'-TCCTCTGACTCAACAGCGAC-3' and 5'-GCTGTAGCCAAATTCGTGTCA-3'). qRT-PCR was performed using the QuantStudio 5 Real-Time PCR System, and the Ct values of *Ntcp* were normalized to the mean values obtained using *Gapdh* as a housekeeping gene ( $\Delta\Delta Ct$  method).

## 2.8. Infection experiments with HDV particles enveloped with HBV or DCH L proteins

Hepatitis D virus (HDV) particles enveloped with HBV or DCH L proteins were produced as described previously (Sureau et al., 1992; Takeuchi et al., 2019). Briefly, Huh7 cells ( $3.3 \times 10^5$ ) were cotransfected with 1  $\mu$ g pSVL (D3) plasmid together with 1  $\mu$ g pBS HBV-L, pBS DCH (Rara)-L or pBS DCH (Sydney) L plasmids using TransIT-X2 Dynamic Delivery System in Opti-MEM I Reduced Serum Medium. At 96 h after transfection, supernatants were centrifuged at 3000 rpm for 10 min to remove cellular debris and treated with 4 Unit/mL Turbo DNase (Thermo Fisher Scientific, Cat# AM2239) at 37 °C for 60 min to eliminate the contaminated plasmid DNA. For infection, Huh7 cells stably expressing NTCP ( $1 \times 10^6$ ) were plated in a Celltight C-1 Plate 96F plate. After overnight incubation, cells were infected with same amount of HDV particles in the presence of 5% PEG 8000 (Sigma Aldrich, Cat# P5413-500G). The plates were spinocultured at 1200 $\times$ g for 30 min. After 16 h incubation, the culture media were replaced with fresh media. After six day culture, the level of intracellular HDV RNA was quantified by qRT-PCR using the CellAmp Direct RNA Prep Kit for RT-PCR (Real Time), One Step PrimeScript III RT-qPCR Mix (TaKaRa, Cat# RR600B), forward primer (5'-GGACCCCTCAGCGAACA-3'), reverse primer (5'-CCTAGCATCTCCTCTATCGCTAT-3') and probe (5'-FAM/AGGCGC TTC/ZEN/GAGCGGTAGGAGTAAGA/3IABkFQ-3') (Gudima et al., 2007). The qRT-PCR protocol consisted of 1 cycle at 52 °C for 5 min and 95 °C for 10 s, followed by 40 cycles at 95 °C for 5 s, and 60 °C for 30 s. The measurement was performed using the QuantStudio 5 Real-Time PCR System (Thermo Fisher Scientific). The pSVL (D3) plasmid was used to generate a standard curve to calculate the copy number of each sample.

## 2.9. Inhibition of preS1 peptide binding by Myrcludex B treatment

Huh7 cells were prepared as described above and were then treated with 1,000, 100, 10, 1, 0.1, 0.01, or 0.001 nM Myrcludex B (Selleck, Cat# P1105) at 37 °C for 1 h. After two washes with DMEM, cells were inoculated with 400 nM FAM-labeled preS1 peptides and incubated at

37 °C for 1 h. The binding of FAM-labeled preS1 peptides was measured as described above. In addition, the cytotoxicity of Myrcludex B was evaluated with the Cell Counting Kit-8 (Dojindo, Cat# CK04) according to the manufacturer's instructions.

## 2.10. Western blotting

To check the expression level of NTCPs, pelleted cells were lysed in M-PER Mammalian Protein Extraction Reagent (Thermo Scientific, Cat# 78501). After measuring protein concentration with TaKaRa Bradford Protein Assay Kit (TaKaRa, Cat# T9310A), equal amounts of cellular proteins were treated with PNGase F (NEB, Cat# P0704L) as described previously (Takeuchi et al., 2019). PNGase F-treated samples were mixed with an equal volume of 2  $\times$  Bolt LDS sample buffer (Thermo Fisher Scientific, Cat# B0008) containing 2%  $\beta$ -mercaptoethanol (Bio-Rad, Cat# 1610710) and incubated at 70 °C for 10 min. Expression of HA-tagged NTCPs was evaluated using SimpleWestern Abby (ProteinSimple) with an anti-HA Tag (6E2) mouse monoclonal antibody (CST, Cat# 2367S,  $\times 250$ ) and an Anti-Mouse Detection Module (ProteinSimple, Cat# DM-002). In addition, the amount of input protein was measured using a Total Protein Detection Module (ProteinSimple, Cat# DM-TP01).

## 2.11. Alignment of the regions around residue 158 of NTCPs and phylogenetic analysis

The regions around residues 84–87 and 158 of the NTCPs from 20 animal species were aligned using the MUSCLE algorithm in MEGA X (MEGA Software). The parameters of alignment were: gap open,  $-2.90$ ; gap extend, 0.00; and hydrophobicity multiplier, 1.20.

A phylogenetic tree was built using the alignment of NTCP amino acid sequences retrieved from public databases and the evolutionary analysis was conducted in MEGA X (Kumar et al., 2018; Stecher et al., 2020). The evolutionary history was inferred using the Maximum Likelihood method and JTT matrix-based mode (Jones et al., 1992). Initial trees for the heuristic search were obtained by applying the Neighbor-Joining method to a matrix of pairwise distances estimated using JTT model. A discrete Gamma distribution was used to model evolutionary rate differences among sites. The tree is drawn to scale, with branch lengths measured in the number of substitutions per site.

## 2.12. Calculation of identity of NTCP among animal species

The identity of NTCPs among animal species was calculated using MEGA X (Kumar et al., 2018; Stecher et al., 2020) with a pairwise distance matrix. Analyses were conducted using the Poisson correction model. The rate variation among sites was modeled with a gamma distribution (shape parameter = 5). All ambiguous positions were removed for each sequence pair (pairwise deletion option).

## 2.13. Statistical analysis

Differences in binding or viral RNA levels between two conditions (e.g., between wild type NTCP and mutant NTCP) were evaluated using an unpaired, two-tailed Student's *t*-test. Differences in binding or viral RNA levels between three different conditions (e.g., between wild type, amino acid 158 mutants, and 84–87 mutants) were evaluated by one-way ANOVA, followed by the Tukey test. A  $p \leq 0.05$  was considered statistically significant. Analysis was performed using Prism 9 software v9.1.1 (GraphPad Software).

## 3. Results

### 3.1. Genetic similarity of preS1 between DCH and HBV

We aligned the preS1 sequence of 13 strains of DCH, five strains of

HBV (genotype A, B, C, D, and F), two strains of Arctic ground squirrel hepatitis B virus, one strain of woodchuck hepatitis virus and those of other viruses belonging to *Orthohepadnavirus* (Fig. 1A). As expected, HBV has different clades based on the genotype (Fig. 1B), and DCH was also distributed into several clades. Notably, the DCH preS1 sequence is genetically closer to that of HBV rather than that of woodchuck hepatitis virus or Arctic ground squirrel hepatitis B virus, suggesting that DCH preS1 may exhibit a similar function to that of HBV preS1.

### 3.2. Genetic similarity of NTCPs among mammals

We next analyzed the NTCP genetic similarities between human and other animals, including cat (Fig. 2). The phylogenetic tree shows that the cat NTCP is genetically close to primates despite being in a different branch. The similarity rates of human and cat were 86% and 82% at the nucleotide and amino acid levels, respectively, based on the estimation of evolutionary differences between sequences (Supplementary Table 2). Higher sequence distances were seen for NTCPs from other mammal species, such as woodchuck, ground squirrel, mouse, rat, and platypus (sequence identities of <80% compared with human NTCP). Nonetheless, some mammals with a higher NTCP distance from humans contained the same amino acid at position 158 (Fig. 2).

### 3.3. The DCH preS1 peptide binds to both cat and human NTCPs

Myristoylated HBV preS1 peptide (47 amino acids in length) can be used to test the binding of preS1 to its counterpart NTCP (Schulze et al., 2010). Therefore, we synthesized HBV and DCH-derived, FAM-labeled, myristoylated preS1 peptides. Huh7 cells transiently expressing either human NTCP (HumanNTCP) or cat NTCP (CatNTCP) were tested for binding to myristoylated preS1 peptides. To distinguish between transfected and untransfected cells, we cotransfected a plasmid encoding mCherry2 fluorescent protein (Fig. 3A) and measured the percentage of FAM-positive cells in the mCherry2-positive population, which should express each NTCP molecule, via fluorescent microscopy and flow cytometry (Supplementary Fig. 1). The expression level of HA-tagged NTCP molecules was confirmed with western blotting (Fig. 3B). We tested the optimal concentration of preS1 peptide for the binding assay and observed a marginal binding of 400 nM HBV-derived preS1 peptides to control Huh7 cells (Supplementary Fig. 2). In contrast, 400 nM HBV-derived preS1 peptide efficiently bound to Huh7 cells expressing HumanNTCP (Supplementary Fig. 2). Therefore, we used 400 nM of preS1 peptides for further experiments (Fig. 3C and D). The binding was not observed with the HBV-derived preS1 peptide harboring the N9K substitution (Fig. 3D), which is consistent with previous studies demonstrating that the N9 residue is critical for interaction with HumanNTCP (Yan et al., 2012). The HBV-derived preS1 peptide showed significant binding to CatNTCP to a level similar to that of HumanNTCP (Fig. 3C and D). This result was confirmed with Huh7 cells stably expressing HumanNTCP or CatNTCP (Supplementary Fig. 3A, 3B and 3C). As previously described (Takeuchi et al., 2019), cynomolgus monkey NTCP (CmNTCP) did not support the binding of the HBV-derived preS1 peptide. Furthermore, we found that the DCH-derived preS1 peptide efficiently bound to both CatNTCP and HumanNTCP but not to CmNTCP (Fig. 3C and D and Supplementary Fig. 2). Similar to the HBV preS1 peptide, the DCH-derived preS1 peptide harboring the N9K substitution failed to bind to any NTCPs (Fig. 3C and D, Supplementary Figs. 3B and 3C).

To test the breadth of the DCH preS1 peptide binding, we expanded our analysis to NTCP molecules from other mammals, including squirrel monkey, Nancy Ma's night monkey, tiger, Geoffroy's cat, dog, horseshoe bat, black fruit bat, pig, cow, treeshrew, woodchuck, ground squirrel, mouse, rat, and platypus (Figs. 2 and 4A). Notably, squirrel monkey, horseshoe bat, ground squirrel, and woodchuck are natural hosts for *Orthohepadnavirus* species (Magnius et al., 2020). The DCH-derived preS1 peptide bound to NTCP from a wide range of mammals (Fig. 4B

and C). Although possible transmission cases of DCH to dogs have been reported (Choi et al., 2022; Diakoudi et al., 2022), the binding of the DCH-derived preS1 peptide to dog NTCP was weak. Collectively, both HumanNTCP and CatNTCP are binding molecules for the DCH-derived preS1 peptide.

### 3.4. Cat and human NTCPs are functional receptors for DCH

To elucidate the functional interaction between DCH envelope L protein and NTCP molecules, we performed an infection assay using HDV particles enveloped with L proteins derived from HBV, DCH (Rara) or DCH (Sydney). Consistent with previous studies (Sureau et al., 1992; Takeuchi et al., 2019), HDV particles enveloped with HBV L protein infected Huh7 cells expressing HumanNTCP (Fig. 5A). Notably, HDV particles enveloped with L proteins derived from DCH (Rara) or DCH (Sydney) established infection on Huh7 cells stably expressing either HumanNTCP or CatNTCP.

Furthermore, we used primary human hepatocytes (PHHs) to test preS1 peptide binding and the infections of HDV particles enveloped with L proteins derived from HBV, DCH (Rara) or DCH (Sydney). Although we observed a slight binding of the N9K mutant peptide, the HBV-derived preS1 peptide efficiently bound to PHHs (Fig. 5B). We performed a knockdown of *Ntcp* in PHHs to see the role of NTCP on preS1 peptide binding. While we observed a decreased level of *Ntcp* mRNA (Supplementary Fig. 4), the effect of *Ntcp* knockdown on preS1 peptide binding was minimal (Fig. 5B). We failed to detect specific binding of the DCH-derived preS1 peptide to PHHs under our experimental condition. Nevertheless, HDV particles enveloped with L proteins derived from HBV or DCH (Rara) established infection in PHHs (Fig. 5C), suggesting that DCH (Rara) can utilize HumanNTCP as a functional receptor.

These observations suggest that HumanNTCP and CatNTCP are functional receptors for DCH.

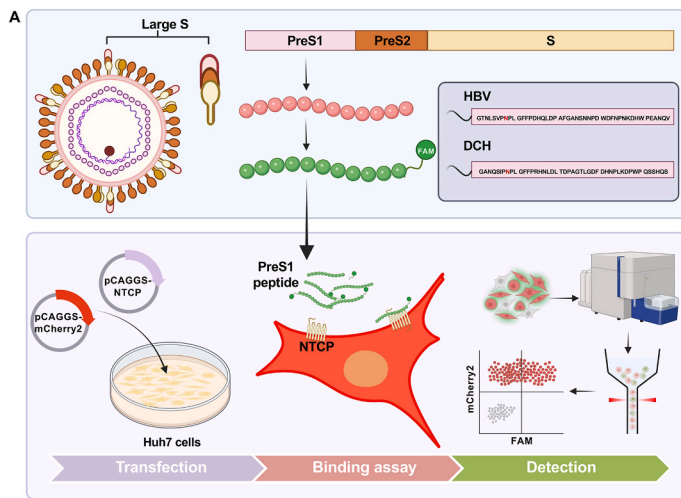
### 3.5. The G158 residue of NTCP determines species specificity of the DCH preS1 peptide binding

Previous studies demonstrated that G158 of HumanNTCP is critical for interaction with the HBV-derived preS1 peptide (Takeuchi et al., 2019). To evaluate whether this applies to the DCH-derived preS1 peptide, we generated mutant NTCPs including HumanNTCP (G158R), CatNTCP (G158R), and CmNTCP (R158G) (Fig. 6A). The HBV-derived preS1 peptide lost binding to HumanNTCP (G158R) and CatNTCP (G158R) but acquired significant binding to CmNTCP (R158G) (Fig. 6B, C and D). Similarly, the DCH-derived preS1 peptide lost binding to HumanNTCP (G158R) and CatNTCP (G158R) (Fig. 6B, C and D). While the DCH-derived preS1 peptide did not show significant binding to CmNTCP (R158G), these observations suggest that the binding pattern of the DCH-derived preS1 peptide to HumanNTCP and CatNTCP is similar to that of the HBV-derived preS1 peptide. The amino acid at position 158 is therefore critical for binding with the DCH-derived preS1 peptide. Furthermore, we tested whether 84–87th amino acids derived from human or mouse NTCPs affect the binding of HBV or DCH preS1 peptides since previous studies demonstrated that this domain determines the tropism of HBV with mouse NTCP (He et al., 2016; Yan et al., 2013). Consistent with the previous study, swapping 84–87th amino acids of human NTCP (RLKN) with that of mouse NTCP (HLTS) decreased the binding of HBV-derived preS1 peptide (Fig. 6B, C and D). In contrast, swapping this domain abolished the binding of DCH-derived preS1 peptide, suggesting that interaction with mouse NTCP may differ between HBV-derived and DCH-derived preS1 peptides.

In addition to CmNTCP (R158), non-G residues at this position can be found in NTCP of animals such as Nancy Ma's night monkey (S158), Geoffroy's cat (S158), pig (S158), and black fruit bat (E158) (Fig. 2). Binding analyses demonstrated that these NTCPs do not support binding of either the HBV-derived or the DCH-derived preS1 peptides (Fig. 4B

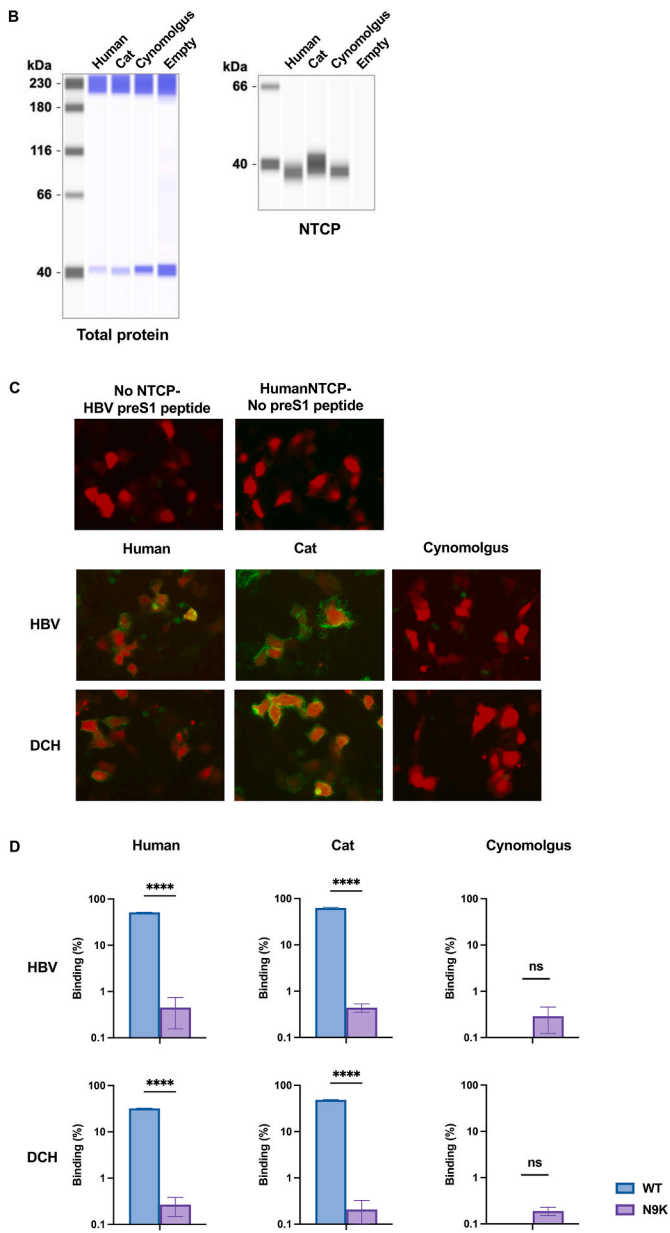






**Fig. 3.** HBV and DCH preS1 peptides bind to both CatNTCP and HumanNTCP but not to CmNTCP.

(A) Schematic overview of the binding assay of FAM-labeled preS1 peptides to Huh7 cells cotransfected with human, cat, or cynomolgus monkey NTCPs and mCherry2-expressing plasmid. For analyses with fluorescent microscopy or a flow cytometer, the presence of FAM-positive cells in the mCherry2-positive population was analyzed. (B) Expression levels of human, cat, or cynomolgus monkey NTCPs in transiently transfected Huh7 cells were examined via western blotting. (C) Huh7 cells transiently expressing NTCPs were inoculated with 400 nM HBV or DCH-derived preS1 peptides. HumanNTCP-expressing cells without the HBV-derived preS1 peptide and normal Huh7 cells inoculated with the HBV-derived preS1 peptide were negative controls. (D) Huh7 cells transiently expressing NTCPs were inoculated with 400 nM HBV or DCH-derived preS1 peptides harboring wild-type amino acids or N9K substitution. The binding of HBV or DCH-derived preS1 peptides to NTCPs was measured via flow cytometry. Differences in binding between wild type and N9K peptides were evaluated using an unpaired, two-tailed Student's *t*-test. \*\*\*\**p* < 0.0001, ns (not significant).



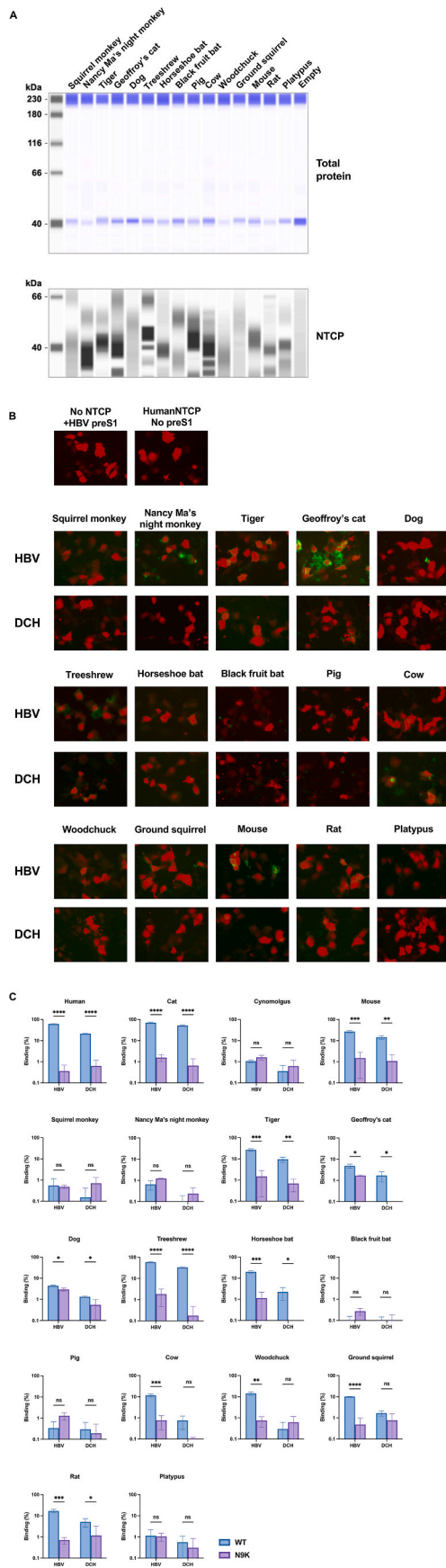


**Fig. 4.** The binding spectrum of the DCH-derived preS1 peptide to mammalian NTCPs.

(A) Expression levels of mammalian NTCPs in transiently transfected Huh7 cells were examined via western blotting. (B) Huh7 cells transiently expressing NTCPs were inoculated with 400 nM HBV or DCH-derived preS1 peptides. HumanNTCP-expressing cells without the HBV-derived preS1 peptide and normal Huh7 cells inoculated with the HBV-derived preS1 peptide were negative controls. (C) Huh7 cells transiently expressing NTCPs were inoculated with 400 nM HBV or DCH-derived preS1 peptides harboring wild-type amino acids or N9K substitution. Binding of HBV or DCH-derived preS1 peptides to NTCPs was measured via flow cytometry. Differences in binding between wild type and N9K peptides were evaluated using an unpaired, two-tailed Student's *t*-test. \*\*\*\**p* < 0.0001, \*\*\**p* < 0.001, \*\**p* < 0.01, \**p* < 0.05, ns (not significant).

species suggests that several strains of DCH are genetically closer to HBV than *Orthohepadnavirus* associated with other host species. This suggests that DCH infection in cats can be a promising animal model for HBV infection. However, infectious DCH has yet to be isolated, and this should be a focus of continued research, specifically in cats. It is critical to understand whether the pathogenesis of DCH in infected cats causes chronic hepatitis and hepatocellular carcinoma as HBV infection can do in humans. Furthermore, although an analysis based on a naturally infected cat suggested a low possibility of sexual transmission of DCH (Capozza et al., 2021), this should be evaluated under controlled experimental conditions.

We identified CatNTCP as a binding molecule for the preS1 peptide of DCH (Fig. 3), and as a functional receptor for HDV particles enveloped with DCH L proteins (Fig. 5A and C), suggesting that CatNTCP is a cellular receptor for DCH. Furthermore, mutagenesis of glycine at NTCP position 158 to arginine caused a loss in binding to the DCH-derived preS1 peptide for both HumanNTCP (G158R) or CatNTCP (G158R) (Fig. 6B and C), indicating the shared nature of the binding of DCH- and HBV-derived preS1 peptide to the NTCP receptors. Furthermore, DCH may be zoonotic in some circumstances as the DCH-derived preS1 peptide efficiently bound to NTCPs from a broad animal species, including humans (Fig. 4B and C). However, infectious DCH culture is required to enable testing of DCH replication in human cells. Interestingly, dog NTCP minimally supported the binding of the HBV-derived and the DCH-derived preS1 peptides (Fig. 4B and C). Although DCH has been identified in dogs (Diakoudi et al., 2022), the low level of expression of dog NTCP in our system might contribute to this discrepancy and should be evaluated in future experiments.

Myrcludex B efficiently inhibited the interaction of the DCH-derived preS1 peptide with CatNTCP (Fig. 7B), suggesting that Myrcludex B can be used for treating cats chronically infected with DCH. Furthermore, clinical information from DCH-infected cats may provide insights for control of HBV infection and eliminating DCH from persistently infected cats could contribute to advances in HBV cure.

A previous study demonstrated that several amino acids of NTCP were under positive selection (Jacquet et al., 2019; Takeuchi et al., 2019), suggesting that NTCP has been a frontline for cell invasion by viruses, especially hepadnaviruses. Intriguingly, CmNTCP encodes R158 to provide an escape from infection with HBV. We demonstrated that non-G residues were present at amino acid 158 of NTCP in several animal species (Fig. 2A), and it would be interesting to investigate whether these species are natural hosts for *Orthohepadnavirus* and, if so, whether coevolution of their preS1 sequence has occurred to compensate for the decreased binding caused by the non-G residue at NTCP position 158. Another possible evolutionary tactic would be using a different receptor molecule to infect the host in these species. Furthermore, in addition to NTCP, the species tropism of *Orthohepadnavirus* should be determined by positive or negative host factors that enhance or inhibit viral replication. Testing these possibilities will provide essential insights into the arms race between hepadnaviruses and mammals.

The HBV-like virus has been identified in pigs (Vieira et al., 2014). However, the genetic distance between HBV and HBV-like viruses in

(caption on next column)



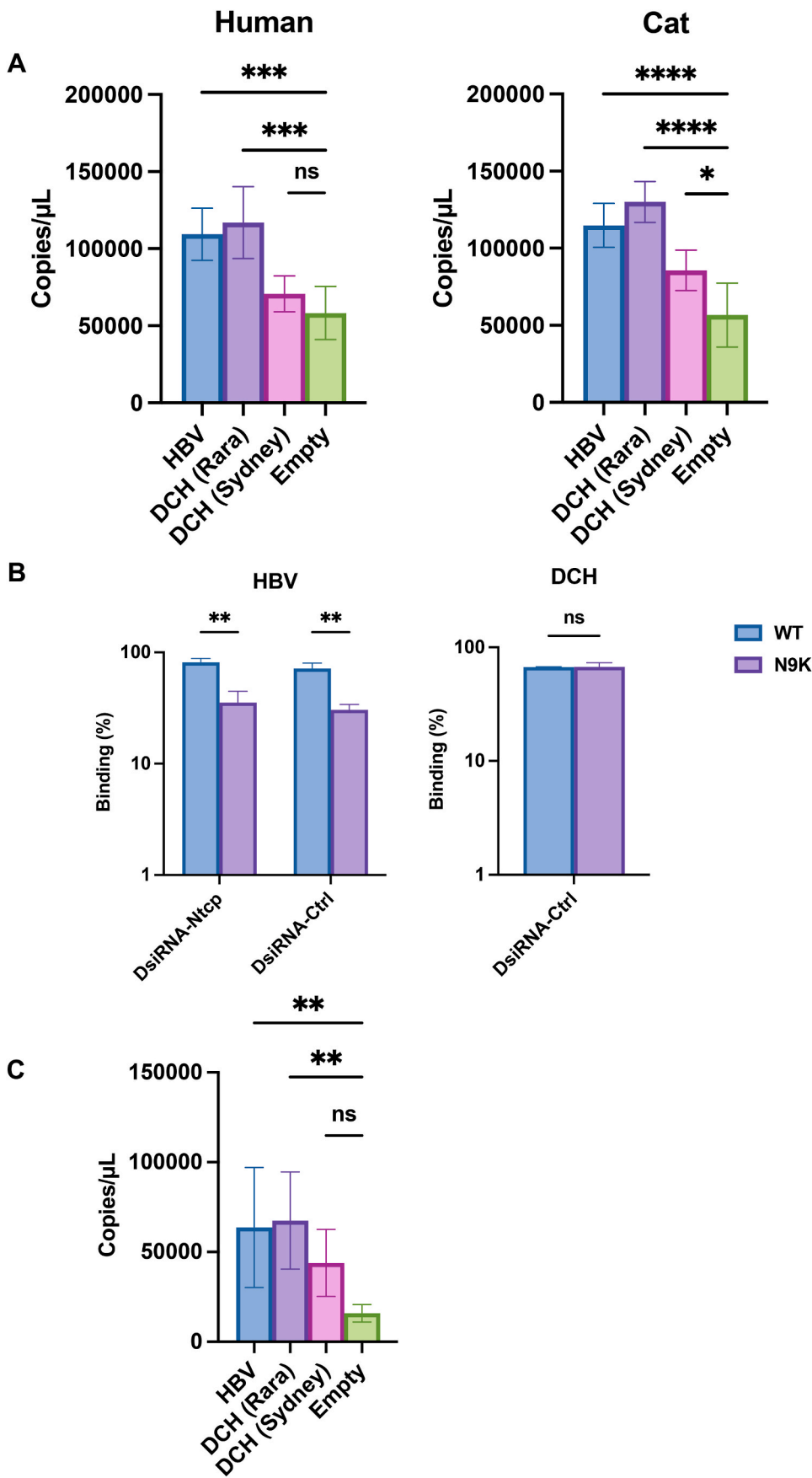
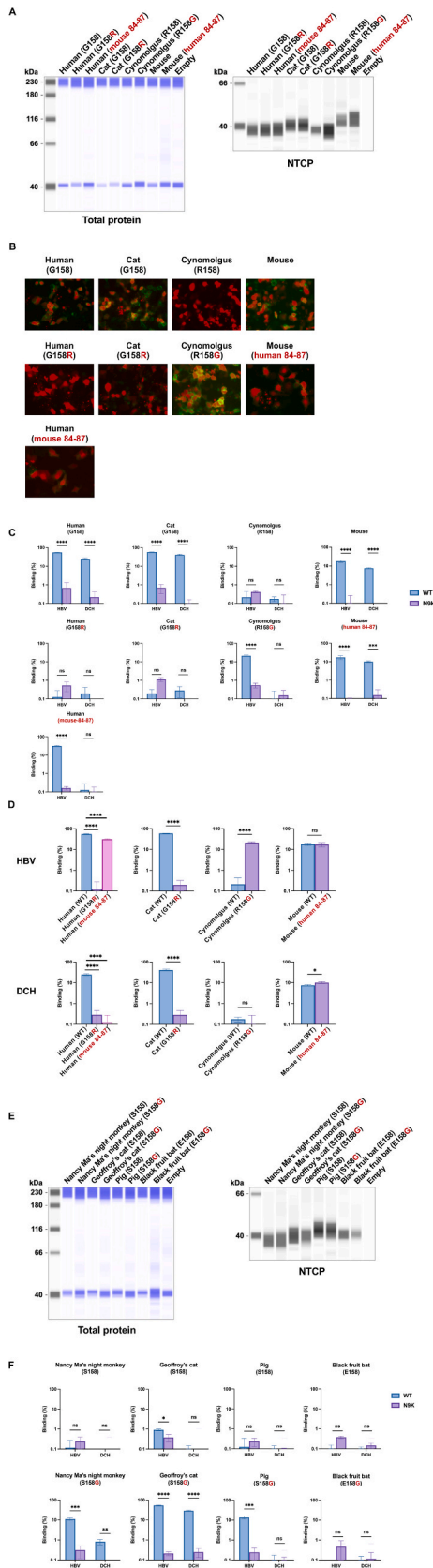


Fig. 5. CatNTCP is a functional receptor for DCH.

(A) Replication of HDV particles enveloped with L proteins derived from HBV, DCH (Rara) or DCH (Sydney) in Huh7 cells stably expressing HumanNTCP or CatNTCP. Differences in viral RNA levels between HBV, DCH (Rara), DCH (Sydney) or Empty were evaluated by one-way ANOVA, followed by the Tukey test. \*\*\*\* $p < 0.0001$ , \*\*\* $p < 0.001$ , \* $p < 0.05$ , ns (not significant). (B) Primary human hepatocytes (PHHs) were transfected with DsiRNA targeting *Ntcp* (left) or non-targeting control DsiRNA (right). Cells were inoculated with 1000 nM HBV or DCH-derived preS1 peptides harboring wild-type amino acids or N9K substitution. The binding of HBV or DCH-derived preS1 peptides to NTCPs was measured via flow cytometry. Differences in binding between wild type and N9K peptides were evaluated using an unpaired, two-tailed Student's *t*-test. \*\* $p < 0.01$ , ns (not significant). (C) Replication of HDV particles enveloped with L proteins derived from HBV, DCH (Rara) or DCH (Sydney) in PHHs. Differences in viral RNA levels between HBV, DCH (Rara), DCH (Sydney) or Empty were evaluated by one-way ANOVA, followed by the Tukey test. \*\* $p < 0.01$ , ns (not significant).



**Fig. 6.** The G158 residue of NTCP determines the species specificity of the DCH preS1 peptide binding. (A) Expression levels of human (G158, WT; G158R), Cat (G158, WT; G158R), cynomolgus monkey (R158, WT; R158G) NTCPs in transiently transfected Huh7 cells examined via western blotting. (B) Huh7 cells transiently expressing NTCPs were inoculated with 400 nM HBV or DCH-derived preS1 peptides. HumanNTCP-expressing cells without the HBV-derived preS1 peptide and normal Huh7 cells inoculated with the HBV-derived preS1 peptide were negative controls. (C) Huh7 cells transiently expressing NTCPs were inoculated with 400 nM HBV or DCH-derived preS1 peptides harboring wild type amino acids or N9K substitution. The binding of HBV or DCH-derived preS1 peptides to NTCPs was measured via flow cytometry. The results are presented as the mean and standard deviation of triplicate measurements from one assay, and they are representative of at least three independent experiments. Differences in binding between wild type and N9K peptides were evaluated using an unpaired, two-tailed Student's *t*-test. \*\*\*\**p* < 0.0001, \*\*\**p* < 0.001, ns (not significant). (D) The data shown in Fig. 6C were used for the statistical analysis. Differences in HBV- or DCH-derived preS1 peptides binding between wild type, amino acid 158 mutants, and 84–87 mutants were evaluated by one-way ANOVA, followed by the Tukey test. \*\*\*\**p* < 0.0001, \**p* < 0.05, ns (not significant). (E) Expression levels of Nancy Ma's night monkey (S158, WT; S158G), Geoffroy's cat (S158, WT; S158G), pig (S158, WT; S158G), black fruit bat (E158, WT; E158G) NTCPs in transiently transfected Huh7 cells were examined via western blotting. (F) Huh7 cells transiently expressing NTCPs were inoculated with 400 nM HBV or DCH-derived preS1 peptides harboring wild type amino acids or N9K substitution. The binding of HBV or DCH-derived preS1 peptides to NTCPs was measured via flow cytometry. The results are presented as the mean and standard deviation of triplicate measurements from one assay, and they are representative of at least three independent experiments. Differences in binding between wild type and N9K peptides were evaluated using an unpaired, two-tailed Student's *t*-test. \*\*\*\**p* < 0.0001, \*\*\**p* < 0.001, \*\**p* < 0.01, \**p* < 0.05, ns (not significant).

pigs is very close, which may be possible contamination of viral DNA from HBV-infected humans. Our analysis demonstrated that the HBV-derived preS1 peptide did not bind to pig NTCP, supporting this hypothesis. Alternatively, the HBV-like virus in pigs may carry other mutations in the preS1 domain for efficient binding with pig NTCP harboring S158. A previous study showed that pig hepatocytes support HBV replication if the entry step is bypassed by the expression of human NTCP (Lempp et al., 2017). Considering the risk of food-borne transmission, whether pigs can be a host for *Orthohepadnavirus* species should be investigated.

A limitation of this study is that we used synthesized lipopeptides to test the interaction between preS1 and the NTCP molecules and investigate the viral entry pathway. While we showed that HDV particles enveloped with L proteins derived from DCH (Rara) or DCH (Sydney) established infection on Huh7 cells expressing either HumanNTCP or CatNTCP, the interaction between the DCH and NTCPs requires experimental verification using an infectious virus. Consequently, we are currently trying to isolate infectious DCH. We believe future studies using infectious DCH will support our present findings.

In conclusion, we revealed a significant similarity in the cell entry pathway between HBV and DCH, suggesting a potential risk of inter-species transmission. Furthermore, our finding that Myrcludex B is active against both HBV and DCH suggests that the DCH infection in cats can be a promising animal model for HBV research.

**Contributions**

M.S. and A.S. designed experiments. M.S., A.O., and A.S. performed experiments. M.S. Y.K., and A.S. analyzed results. M.S. and A.S. wrote the manuscript. All authors read and approved the manuscript.

**Funding**

This work was supported by grants from the Japan Agency for Medical Research and Development (AMED) Research Program on HIV/

(caption on next column)

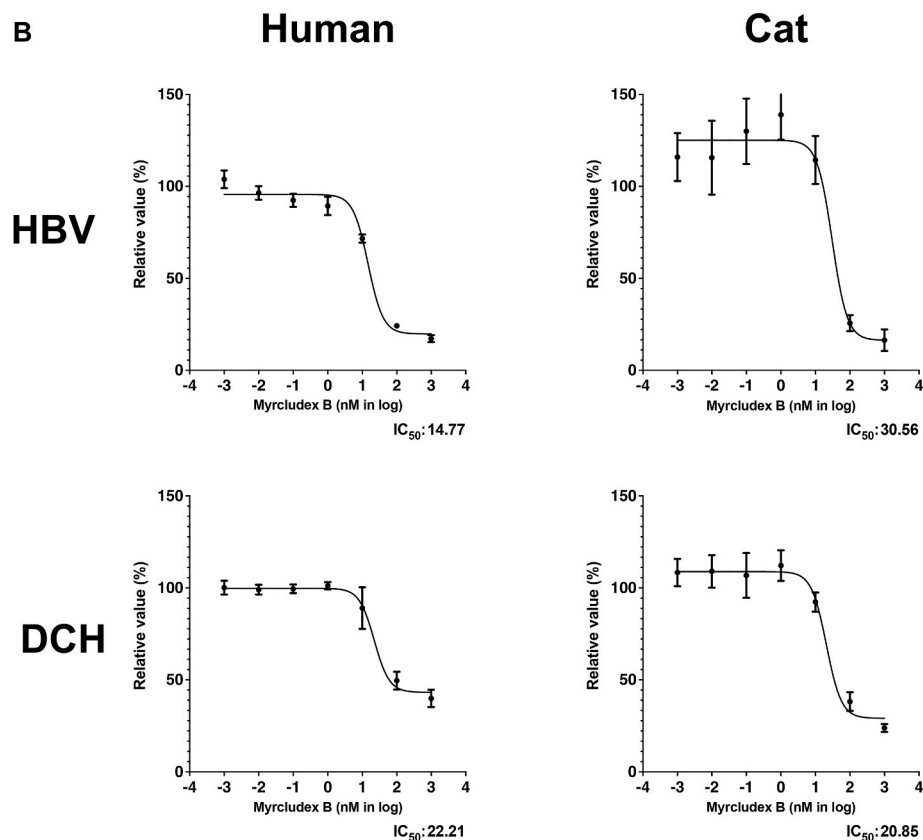
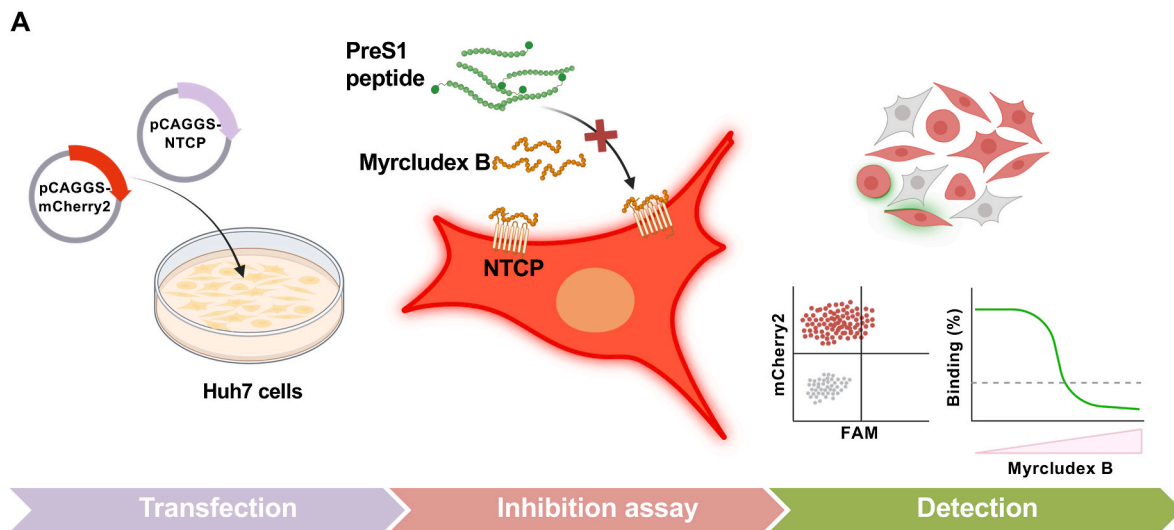


**Fig. 7.** Myrcludex B treatment blocks the binding of the DCH preS1 peptide to both human and cat NTCPs.

(A) Schematic overview of the Myrcludex B-mediated inhibition assay using 400 nM FAM-labeled PreS1 peptides to Huh7 cells cotransfected with human or cat NTCPs and a mCherry2-expressing plasmid. For analyses with fluorescent microscopy or a flow cytometer, the percentage of FAM-positive cells in the mCherry2-positive population was analyzed. (B) Myrcludex B inhibits the binding of HBV or DCH-derived preS1 peptides to human or cat NTCPs; IC<sub>50</sub> values were calculated.

AIDS JP22fk0410033 and JP22fk0410047 (to A.S.); AMED Research Program on Emerging and Re-emerging Infectious Diseases JP21fk0108425, JP21fk0108465, and JP21fk0108481 (to A.S.); AMED Japan Program for Infectious Diseases Research and Infrastructure JP22wm0325009 (to A.S.); AMED CRDF Global Grant JP22jk0210039 (to A.S.); from JSPS KAKENHI Grant-in-Aid for Scientific Research (B) 22H02500 (to A.S.) and from the Ito Foundation Research Grant R4 KEN132 (to A.S.).

#### Declaration of competing interest

The authors declare that they have no known competing financial interests or personal relationships that could have appeared to influence the work reported in this paper.

#### Data availability

Data will be made available on request.

## Acknowledgements

The authors thank Dr. Toru Okamoto (Juntendo University) for insightful suggestions and for providing the pBS HBV-L plasmid. The following reagents were obtained through the Addgene: pMD2.G was a gift from Dr. Didier Trono and pSVL (D3) was a gift from Dr. John Taylor. The psPAX2-IN/HiBiT plasmid was a kind gift from Dr. Kenzo Tokunaga. The authors thank Ms. Tomoko Nishiuchi and Ms. Yuki Shibata for their assistance. This study was supported by the Frontier Science Research Center, University of Miyazaki. Figs. 2, 3A and 7A were created with BioRender (<https://biorender.com/>).

## Glossary

DCH	Domestic cat hepadnavirus
HBV	Hepatitis B virus
NTCP	sodium/bile acid cotransporter
MEGA	Molecular Evolutionary Genetics Analysis

## Appendix A. Supplementary data

Supplementary data to this article can be found online at <https://doi.org/10.1016/j.antiviral.2023.105695>.

## References

- Aghazadeh, M., Shi, M., Barrs, V.R., McLuckie, A.J., Lindsay, S.A., Jameson, B., Hampson, B., Holmes, E.C., Beatty, J.A., 2018. A novel hepadnavirus identified in an immunocompromised domestic cat in Australia. *Viruses* 10, 269. <https://doi.org/10.3390/v10050269>.
- Alting-Mees, M.A., Short, J.M., 1989. pBluescript II: gene mapping vectors. *Nucleic Acids Res.* 17, 9494. <https://doi.org/10.1093/nar/17.22.9494>.
- Anpuanandam, K., Selvarajah, G.T., Choy, M.M.K., Ng, S.W., Kumar, K., Ali, R.M., Rajendran, S.K., Ho, K.L., Tan, W.S., 2021. Molecular detection and characterisation of Domestic Cat Hepadnavirus (DCH) from blood and liver tissues of cats in Malaysia. *BMC Vet. Res.* 17, 9. <https://doi.org/10.1186/s12917-020-02700-0>.
- Capozza, P., Carrai, M., Choi, Y.R., Tu, T., Nekouei, O., Lanave, G., Martella, V., Beatty, J.A., Barrs, V.R., 2023. Domestic cat hepadnavirus: molecular epidemiology and phylogeny in cats in Hong Kong. *Viruses* 15, 150. <https://doi.org/10.3390/v15010150>.
- Capozza, P., Lanave, G., Diakoudi, G., Stasi, F., Ghergo, P., Ricci, D., Santo, G., Arena, G., Grillo, I., Delle Donne, E., Di Liso, F., Zini, E., Callegari, C., Valente, L., Camero, M., Di Martino, B., Beatty, J., Barrs, V.R., Buonavoglia, C., Martella, V., 2021. A longitudinal observational study in two cats naturally-infected with hepadnavirus. *Vet. Microbiol.* 254, 108999. <https://doi.org/10.1016/j.vetmic.2021.108999>.
- Choi, Y.R., Chen, M.-C., Carrai, M., Rizzo, F., Chai, Y., Tse, M., Jackson, K., Martella, V., Steiner, J., Pesavento, P.A., Beatty, J.A., Barrs, V.R., 2022. Hepadnavirus DNA is detected in canine blood samples in Hong Kong but not in liver biopsies of chronic hepatitis or hepatocellular carcinoma. *Viruses* 14, 1543. <https://doi.org/10.3390/v14071543>.
- Delmas, J., Schorr, O., Jamard, C., Gibbs, C., Trépo, C., Hantz, O., Zoulim, F., 2002. Inhibitory effect of adefovir on viral DNA synthesis and covalently closed circular DNA formation in duck hepatitis B virus-infected hepatocytes in vivo and in vitro. *Antimicrob. Agents Chemother.* 46, 425–433. <https://doi.org/10.1128/AAC.46.2.425-433.2002>.
- Diakoudi, G., Capozza, P., Lanave, G., Pellegrini, F., Di Martino, B., Elia, G., Decaro, N., Camero, M., Ghergo, P., Stasi, F., Cavalli, A., Tempesta, M., Barrs, V.R., Beatty, J., Bányai, K., Catella, C., Lucente, M.S., Buonavoglia, A., Fusco, G., Martella, V., 2022. A novel hepadnavirus in domestic dogs. *Sci. Rep.* 12, 2864. <https://doi.org/10.1038/s41598-022-06842-z>.
- Engelke, M., Mills, K., Seitz, S., Simon, P., Gripon, P., Schnölzer, M., Urban, S., 2006. Characterization of a hepatitis B and hepatitis delta virus receptor binding site. *Hepatology* 43, 750–760. <https://doi.org/10.1002/hep.21112>.
- Gripon, P., Cannie, I., Urban, S., 2005. Efficient inhibition of hepatitis B virus infection by acylated peptides derived from the large viral surface protein. *J. Virol.* 79, 1613–1622. <https://doi.org/10.1128/JVI.79.3.1613-1622.2005>.
- Gudima, S., He, Y., Meier, A., Chang, J., Chen, R., Jarnik, M., Nicolas, E., Bruss, V., Taylor, J., 2007. Assembly of hepatitis delta virus: particle characterization, including the ability to infect primary human hepatocytes. *J. Virol.* 81, 3608–3617. <https://doi.org/10.1128/JVI.02277-06>.
- Guo, J.T., Zhou, H., Liu, C., Aldrich, C., Saputelli, J., Whitaker, T., Barrasa, M.I., Mason, W.S., Seeger, C., 2000. Apoptosis and regeneration of hepatocytes during recovery from transient hepadnavirus infections. *J. Virol.* 74, 1495–1505. <https://doi.org/10.1128/jvi.74.3.1495-1505.2000>.
- He, W., Cao, Z., Mao, F., Ren, B., Li, Y., Li, D., Li, H., Peng, B., Yan, H., Qi, Y., Sun, Y., Wang, F., Sui, J., Li, W., 2016. Modification of three amino acids in sodium taurocholate cotransporting polypeptide renders mice susceptible to infection with hepatitis D virus in vivo. *J. Virol.* 90, 8866–8874. <https://doi.org/10.1128/JVI.00901-16>.
- Jacquet, S., Pons, J.-B., De Bernardo, A., Ngoubangoye, B., Cosset, F.-L., Régis, C., Etienne, L., Pontier, D., 2019. Evolution of hepatitis B virus receptor NTCP reveals differential pathogenicities and species specificities of hepadnaviruses in primates, rodents, and bats. *J. Virol.* 93, e01738-18. <https://doi.org/10.1128/JVI.01738-18>.
- Jeanes, E.C., Wegg, M.L., Mitchell, J.A., Priestnall, S.L., Fleming, L., Dawson, C., 2022. Comparison of the prevalence of domestic cat Hepadnavirus in a population of cats with uveitis and in a healthy blood donor cat population in the United Kingdom. *Vet. Ophthalmol.* 25, 165–172. <https://doi.org/10.1111/vop.12956>.
- Jilbert, A.R., Wu, T.T., England, J.M., Hall, P.M., Carp, N.Z., O'Connell, A.P., Mason, W.S., 1992. Rapid resolution of duck hepatitis B virus infections occurs after massive hepatocellular involvement. *J. Virol.* 66, 1377–1388. <https://doi.org/10.1128/JVI.66.3.1377-1388.1992>.
- Jones, D.T., Taylor, W.R., Thornton, J.M., 1992. The rapid generation of mutation data matrices from protein sequences. *Comput. Appl. Biosci.* 8, 275–282. <https://doi.org/10.1093/bioinformatics/8.3.275>.
- Kajino, K., Jilbert, A.R., Saputelli, J., Aldrich, C.E., Cullen, J., Mason, W.S., 1994. Woodchuck hepatitis virus infections: very rapid recovery after a prolonged viremia and infection of virtually every hepatocyte. *J. Virol.* 68, 5792–5803. <https://doi.org/10.1128/JVI.68.9.5792-5803.1994>.
- Kumar, S., Stecher, G., Li, M., Nkayaz, C., Tamura, K., 2018. MEGA X: molecular evolutionary genetics analysis across computing platforms. *Mol. Biol. Evol.* 35, 1547–1549. <https://doi.org/10.1093/molbev/msy096>.
- Kuo, M.Y., Chao, M., Taylor, J., 1989. Initiation of replication of the human hepatitis delta virus genome from cloned DNA: role of delta antigen. *J. Virol.* 63, 1945–1950. <https://doi.org/10.1128/JVI.63.5.1945-1950.1989>.
- Lanave, G., Capozza, P., Diakoudi, G., Catella, C., Catucci, L., Ghergo, P., Stasi, F., Barrs, V., Beatty, J., Decaro, N., Buonavoglia, C., Martella, V., Camero, M., 2019. Identification of hepadnavirus in the sera of cats. *Sci. Rep.* 9, 10668. <https://doi.org/10.1038/s41598-019-47175-8>.
- Le Seyec, J., Chouteau, P., Cannie, I., Guguen-Guillouzo, C., Gripon, P., 1999. Infection process of the hepatitis B virus depends on the presence of a defined sequence in the pre-S1 domain. *J. Virol.* 73, 2052–2057. <https://doi.org/10.1128/JVI.73.3.2052-2057.1999>.
- Lempp, F.A., Wiedtke, E., Qu, B., Roques, P., Chemin, I., Vondran, F.W.R., Le Grand, R., Grimm, D., Urban, S., 2017. Sodium taurocholate cotransporting polypeptide is the limiting host factor of hepatitis B virus infection in macaque and pig hepatocytes. *Hepatology* 66, 703–716. <https://doi.org/10.1002/hep.29112>.
- Magnius, L., Mason, W.S., Taylor, J., Kann, M., Glebe, D., Dény, P., Sureau, C., Norder, H., 2020. ICTV virus taxonomy profile: hepadnaviridae. *J. Gen. Virol.* 101, 571–572. <https://doi.org/10.1099/jgv.0.001415>.
- Marion, P.L., Salazar, F.H., Winters, M.A., Colonno, R.J., 2002. Potent efficacy of entecavir (BMS-200475) in a duck model of hepatitis B virus replication. *Antimicrob. Agents Chemother.* 46, 82–88. <https://doi.org/10.1128/AAC.46.1.82-88.2002>.
- Niwa, H., Yamamura, K., Miyazaki, J., 1991. Efficient selection for high-expression transfectants with a novel eukaryotic vector. *Gene* 108, 193–199. [https://doi.org/10.1016/0378-1119\(91\)90434-d](https://doi.org/10.1016/0378-1119(91)90434-d).
- Ozono, S., Zhang, Y., Tobiume, M., Kishigami, S., Tokunaga, K., 2020. Super-rapid quantitation of the production of HIV-1 harboring a luminescent peptide tag. *J. Biol. Chem.* 295, 13023–13030. <https://doi.org/10.1074/jbc.RA120.013887>.
- Petersen, J., Dandri, M., Mier, W., Lütgehettmann, M., Volz, T., von Weizsäcker, F., Haberkorn, U., Fischer, L., Pollok, J.-M., Erbes, B., Seitz, S., Urban, S., 2008. Prevention of hepatitis B virus infection in vivo by entry inhibitors derived from the large envelope protein. *Nat. Biotechnol.* 26, 335–341. <https://doi.org/10.1038/nbt1389>.
- Piewbang, C., Wardhani, S.W., Chaiyasak, S., Yostawonkul, J., Chai-In, P., Boonrungsiman, S., Kasantikul, T., Techangamsuwan, S., 2020. Insights into the genetic diversity, recombination, and systemic infections with evidence of intracellular maturation of hepadnavirus in cats. *PLoS One* 15, e0241212. <https://doi.org/10.1371/journal.pone.0241212>.
- Schulze, A., Schieck, A., Ni, Y., Mier, W., Urban, S., 2010. Fine mapping of pre-S sequence requirements for hepatitis B virus large envelope protein-mediated receptor interaction. *J. Virol.* 84, 1989–2000. <https://doi.org/10.1128/JVI.01902-09>.
- Stecher, G., Tamura, K., Kumar, S., 2020. Molecular evolutionary genetics analysis (MEGA) for macOS. *Mol. Biol. Evol.* 37, 1237–1239. <https://doi.org/10.1093/molbev/msz312>.
- Stone, C., Petch, R., Gagne, R.B., Nehring, M., Tu, T., Beatty, J.A., VandeWoude, S., 2022. Prevalence and genomic sequence analysis of domestic cat hepadnavirus in the United States. *Viruses* 14, 2091. <https://doi.org/10.3390/v14102091>.
- Sureau, C., Moriarty, A.M., Thornton, G.B., Lanford, R.E., 1992. Production of infectious hepatitis delta virus in vitro and neutralization with antibodies directed against hepatitis B virus pre-S antigens. *J. Virol.* 66, 1241–1245. <https://doi.org/10.1128/JVI.66.2.1241-1245.1992>.
- Takahashi, K., Kaneko, Y., Shibana, A., Yamamoto, S., Katagiri, A., Osuga, T., Inoue, Y., Kuroda, K., Tanabe, M., Okabayashi, T., Naganobu, K., Minobe, I., Saito, A., 2022. Identification of domestic cat hepadnavirus from a cat blood sample in Japan. *J. Vet. Med. Sci.* 84, 648–652. <https://doi.org/10.1292/jvms.22-0010>.
- Takeuchi, J.S., Fukano, K., Iwamoto, M., Tsukuda, S., Suzuki, R., Aizaki, H., Muramatsu, M., Wakita, T., Sureau, C., Watashi, K., 2019. A single adaptive mutation in sodium taurocholate cotransporting polypeptide induced by hepadnaviruses determines virus species specificity. *J. Virol.* 93, e01432-18. <https://doi.org/10.1128/JVI.01432-18>.
- Vieira, Y.R., dos Santos, D.R.L., Portilho, M.M., Velloso, C.E.P., Arissawa, M., Villar, L.M., Pinto, M.A., de Paula, V.S., 2014. Hepadnavirus detected in bile and liver samples

- from domestic pigs of commercial abattoirs. *BMC Microbiol.* 14, 315. <https://doi.org/10.1186/s12866-014-0315-2>.
- Yan, H., Peng, B., He, W., Zhong, G., Qi, Y., Ren, B., Gao, Z., Jing, Z., Song, M., Xu, G., Sui, J., Li, W., 2013. Molecular determinants of hepatitis B and D virus entry restriction in mouse sodium taurocholate cotransporting polypeptide. *J. Virol.* 87, 7977–7991. <https://doi.org/10.1128/JVI.03540-12>.
- Yan, H., Zhong, G., Xu, G., He, W., Jing, Z., Gao, Z., Huang, Y., Qi, Y., Peng, B., Wang, H., Fu, L., Song, M., Chen, P., Gao, W., Ren, B., Sun, Y., Cai, T., Feng, X., Sui, J., Li, W., 2012. Sodium taurocholate cotransporting polypeptide is a functional receptor for human hepatitis B and D virus. *Elife* 1, e00049. <https://doi.org/10.7554/eLife.00049>.
- Zhang, H., Itoh, Y., Suzuki, T., Ihara, K.-I., Tanaka, T., Haga, S., Enatsu, H., Yumiya, M., Kimura, M., Takada, A., Itoh, D., Shibazaki, Y., Nakao, S., Yoshio, S., Miyakawa, K., Miyamoto, Y., Sasaki, H., Kajita, T., Sugiyama, M., Mizokami, M., Tachibana, T., Ryo, A., Moriishi, K., Miyoshi, E., Kanto, T., Okamoto, T., Matsuura, Y., 2022. Establishment of monoclonal antibodies broadly neutralize infection of hepatitis B virus. *Microbiol. Immunol.* 66, 179–192. <https://doi.org/10.1111/1348-0421.12964>.